THE EFFECT OF THE TITANIUM CONTENT ON THE ACTIVE CORROSION OF FERRITIC CR-STEELS AND AUSTENITIC CR-NI-STEELS IN SULFURIC ACID

Günter Herbsleb

(NASA-TT-F-15994) THE EFFECT OF THE TITANIUM CONTENT ON THE ACTIVE CORROSION OF FERRITIC r-STEELS AND AUSTENITIC Cr-Ni-STEELS IN (Scientific Translation Service) 38 p HC $3.75 CSCL 11F G3/26 N75-10211 Unclas 53151

Translation of "Der Einfluss des Titangehaltes auf die Aktivkorrosion ferritischer Cr-Stähle und austenitischer Cr-Ni-Stähle in Schwefelsäure", Werkstoffe und Korrosion, Vol. 20, No. 9, Sept. 1969, pp. 762-772.

NATIONAL AERONAUTICS AND SPACE ADMINISTRATION
WASHINGTON, D. C. 20546 OCTOBER 1974

STANDARD TITLE PAGE

1. Report No. NASA TT F-15,994	2. Government Accession No.	3. Recipient's Catalog No.
4. Title and Subtitle: THE EFFECT OF THE TITANIUM CONTENT ON THE ACTIVE CORROSION OF FERRITIC CR-STEELS AND AUSTENITIC CR-NI-STEELS IN SULFURIC ACID		5. Report Date: October 1974 6. Performing Organization Code
7. Author(s): Günter Herbsleb		8. Performing Organization Report No. 10. Work Unit No.
9. Performing Organization Name and Address: SCITRAN, Box 5456, Santa Barbara, CA 93108		11. Contract or Grant No. NASw-2483 13. Type of Report and Period Covered: Translation
12. Sponsoring Agency Name and Address: National Aeronautics and Space Administration, Washington, D.C. 20546		14. Sponsoring Agency Code

15. Supplementary Notes

Translation of "Der Einfluss des Titangehaltes auf die Aktivkorrosion ferritischer Cr-Stähle und austenitischer Cr-Ni-Stähle in Schwefelsäure", Werkstoffe und Korrosion, Vol. 20, No. 9, Sept. 1969, pp. 762 - 772.

16. Abstract

The steels of types X5 CrNiMoTi 25 25 and X5 CrNi 18 9 are compared with respect to their behavior in the sensitized state and the corrosion properties are discussed from the standpoint of the chromium depletion theory.

17. Key Words (Selected by Author(s))	18. Distribution Statement
	Unclassified - Unlimited

19. Security Classif. (of this report)	20. Security Classif. (of this page)	21. No. of Pages	22. Price
Unclassified	Unclassified	36	

THE EFFECT OF THE TITANIUM CONTENT ON THE ACTIVE CORROSION OF FERRITIC CR-STEELS AND AUSTENITIC CR-NI-STEELS IN SULFURIC ACID

Günter Herbsleb

1. Introduction

/ 762*

The austenitic Cr-Ni or Cr-Ni-Mo steels, which have their principal application in the passive state as corrosion-resistant materials, are also used in the active state when the corrosion rate is low enough. So far, there have been only a few systematic studies of the active corrosion of such steels. H.-J. Engell and T. Ramachandran [1] found a considerable reduction of the corrosion rate of Cu-containing Cr-Ni steels in the active state, as compared to Cu-free steels and ascribed this phenomenon to a partial covering of the steel surface by copper. W. Schwenk [2] showed that the corrosion rate of 18-8 Cr-Ni steels increased with cathodic polarization and that the maximum corrosion rate was at less noble potentials than the resting potential. This finding was confirmed by G. Herbsleb and W. Schwenk [3] for 18-8 Cr-Ni steels with different Mo contents.

The latter studies also showed that the maximum corrosion rate in the active state and correspondingly, in agreement with E. Brauns, W. Schwenk and H.-E. Bühler [4], the corrosion rate at the active rest potential, are reduced by addition of Mo. This is synonymous with a facilitated transition into the stable passive state. Hydrogen sulfide and sulfur dioxide produce a

* Numbers in the margin indicate pagination in the original foreign text.

strong increase in the corrosion rate and largely eliminate the effect of the alloying elements Cr, Ni and Mo on the corrosion in the active state [3, 5]. In the presence of SO_2 and SO_2, pitting corrosion can occur in the active-passive transition region [3, 6].

Indications of the favorable effect of Ti additions on the active corrosion of the austenitic Cr-Ni steels can be found in the literature [4]. The investigations on ferritic Cr-steels and austenitic Cr-Ni steels, in part with added Mo, described in the following, were intended to determine the effect of Ti on the active corrosion of these steels in sulfuric acid through potentiostatic holding experiments over a wide potential range.

2. Experimental Materials

The experiments were done with steels of the types X8Cr17 (Material No. 4016), X8CrTi17 (Material No. 4510), X5CrNi 18 9 (Material No. 4301), X10CrNiTi 18 9 (Material No. 4541) and X5CrNiMoTi 25 25 (Material No. 4577). Their chemical compositions are shown in Table 1.

Steels 6 to 8 have almost identical contents of C, Cr, Ni, Mo and N, and arranged in order of increasing Ti content. In these steels the stabilization ratio,

$$\frac{\%\ \text{Ti}}{\%\text{C} + \%\text{N}}$$

increases from 5.3 (Steel 6) to 9.2 (Steel 8). Steel 9 differs / 763 from the former steels primarily by the C content, which is lower by a factor of about 2. The stabilization ratio for this steel is between those of Steels 6 and 7.

Table 1. CHEMICAL COMPOSITION OF THE EXPERIMENTAL MATERIALS

Steel No.	Material	Material No.	%C	%N	%Cr	%Ni	%Mo	%Ti	$\frac{\%Ti}{\%C}$	$\frac{\%Ti}{\%C + \%N}$	Heat Treatment
1	X 8 Cr 17	4016	0,120	0,023	17,99	0,22	0,01	—	—	—	3 h 750° C/W
2	X 8 CrTi 17	4510	0,047	0,009	17,60	0,22	0,01	0,61	13,2	10,9	3 h 850° C/W
3	X 8 CrTi 17	4510	0,080	0,011	16,67	0,10	n.b.	0,81	10,1	9,0	3 h 850° C/W
4	X 5 CrNi 18 9	4301	0,040	0,032	18,15	10,20	0,25	—	—	—	30 min 1050° C/W
5	X10 CrNiTi 18 9	4541	0,046	0,006	18,07	10,70	0,26	0,46	10,0	8,9	15 min 1100° C/W
6	X 5 CrNiMoTi 25 25	4577	0,060	0,017	25,80	24,80	2,30	0,41	6,8	5,3	15 min 1100° C/W
7	X 5 CrMoTi 25 25	4577	0,070	0,010	25,27	25,14	1,94	0,53	7,6	6,6	15 min 1100° C/W
8	X 5 CrNiMoTi 25 25	4577	0,057	0,012	24,55	25,07	2,19	0,66	11,6	9,6	15 min 1100° C/W
9	X 5 CrNiMoTi 25 25	4577	0,030	0,015	24,50	25,20	2,05	0,32	8,9	6,3	15 min 1100° C/W

The materials were available as cold-rolled plates with thicknesses between 2 and 10 mm. Samples with surfaces between 1 and 5 cm^2 were cut from them. The heat treatment is indicated in Table 1. Samples of Steels 6 to 9 were heated for 2 hours at 650 ° in air to sensitize them after the solution heat treatment. The heat-treated samples of Steels 1 to 5 were etched in nitric-hydrochloric acid etchant, washed in distilled water and acetone, and used air-passive for the experiments. The heating scale was polished off of the samples of Steels 6 to 9 which were used for the electrochemical experiments. For the determination of the corrosion rates of Steels 1 and 3 in hydrofluoric acid, samples were cut out with a surface of some 25 cm^2 and heat-treated and etched as stated above before the experiments.

The ferritic Steel 1 after heat treatment showed very numerous, irregularly distributed coarse carbides of the type $M_{23}C_6$. The solution-heat-treated austenitic Steel 4 was free of precipitates. The titanium-stabilized Steels 2, 3, and 5 showed numerous coarse titanium carbonitrides of the type MX (1) in the structure after heat treatment. In the Steels 2 and 3 they had also partially precipitated at the grain boundaries or at the former grain boundaries.

As supplied, the Steels 6 to 9 have an austenitic structure (Figure 1). Precipitates of titanium nitride (TiN) could be identified by their angular shape and characteristic yellow color. Stages from gray-white to yellow were often observed. Titanium carbide (TiC) appears in the form of gray-white globular particles. It is probable that the phases described actually represent Ti(C,N) with an excess of either C or N.

---

(1) Basic formula for carbonitride. M = metal (Ti); X = C or N. Carbides and nitrides of the type MX form an unbroken series of solid solutions in the solid state [7].

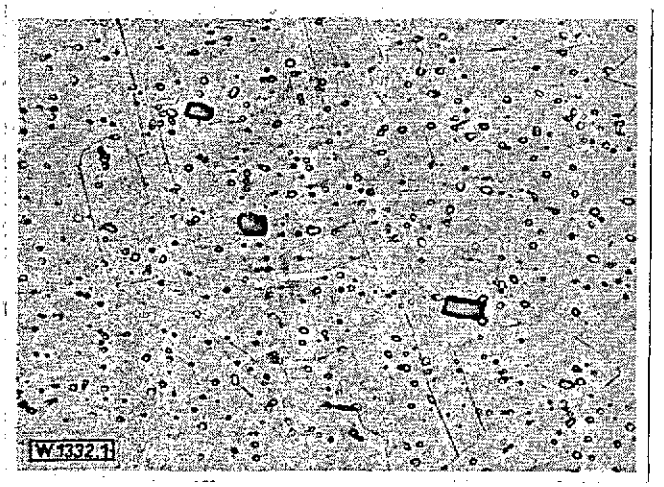

Figure 1. Structure of Steel 6 as furnished with precipitates of TiN and TiC or Ti(C,N) and Ti(C, N). 200:1. V2A etchant.

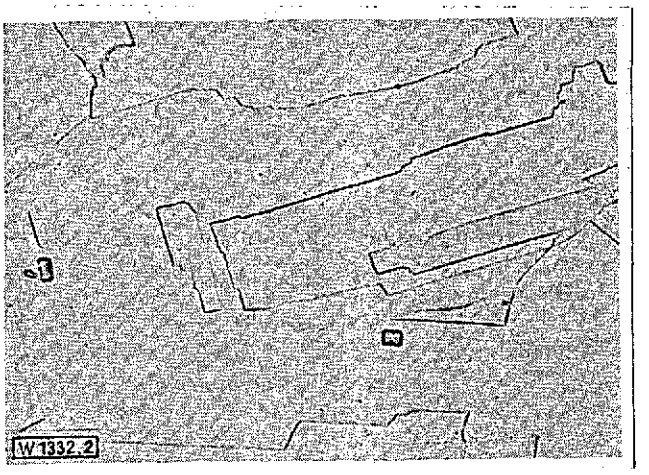

Figure 2. Structure of Steel 6 after solution heat treatment 15 min 1100° C/W with TiN precipitates and (isolated) TiC precipitates. 500:1. Aqua regia + glycerin.

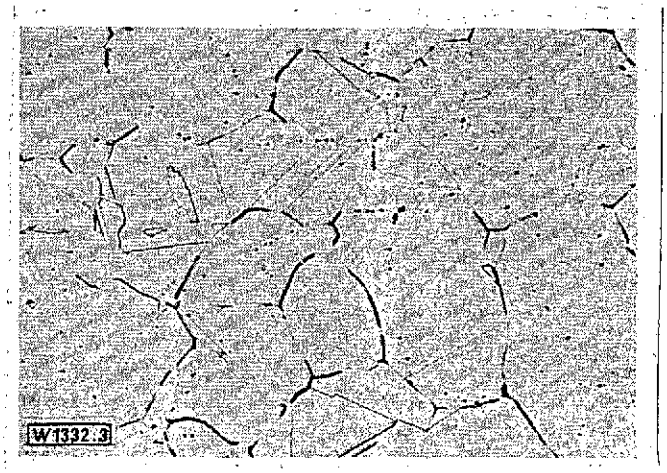

Figure 3. Structure of Steel 8 with grain boundary precipitates after heat treatment 15 min 1100°C/Air. 500:1. V2A etchant.

In many cases Ti(C,N) is surrounded by Ti(C,N) [2] Occasionally precipitates with a three-fold structure are also observed, with an oxide phase colored deep brown at their centers. Investigations of the TiC precipitates with the electron microprobe showed also that in the precipitates the Fe and Ni content are reduced by comparison with the base mass, while the Cr and Mo contents are increased.

After solution heat treatment at high temperatures (1050 to 1150 °C) the number of the gray-white precipitates has decreased considerably (Figure 2). The number of TiN

---

(2) (C,N) designates a phase consisting predominantly of nitride, while (C, N) indicates predominance of the carbide portion.

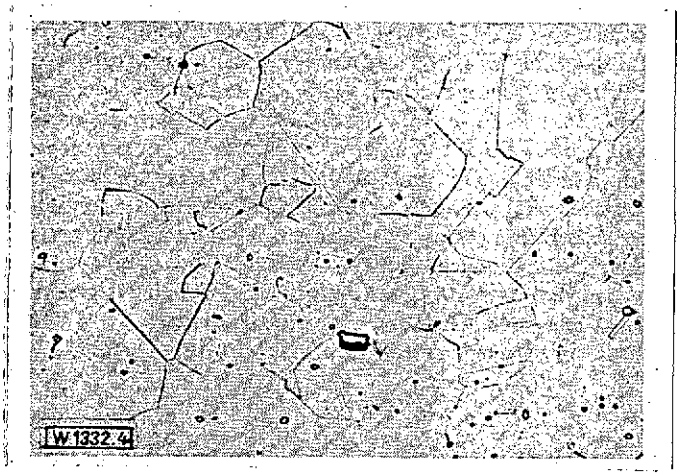

Figure 4. Structure of Steel 9 after heat treatment, 15 min 1100°C/Water + 2 hours 650°C/Air. 500:1. V2A etchant.

precipitates, on the contrary, is not detectably reduced.

On a subsequent sensitizing heating (2 hours 650°C/air) a new formation of grains takes place. The grains do not have the characteristic appearance of an austenitic structure. A typical austenitic structure appears only on strong etching (Figure 3). Steels 6 to 8 show precipitates preferentially on /764
the newly formed and the former grain boundaries (Figure 3). In the grains, more of the TiC phase occurs after the sensitization heating, along with TiN. The grain boundaries of Steel 9 are almost free of precipitates after the sensitization heating (Figure 4).

3. Conduct of the Experiments

All the electrochemical experiments were done in 2 N H_2SO_4 which was made from highest purity concentrated H_2SO_4 by dilution with completely deionized water. The electrolyte was flushed with specially purified nitrogen, from which the remaining oxygen was removed with a copper catalyst down to a residual content of 10^{-5}% O_2 before it was introduced into the test solution. The temperature of the test solution was 60°C.

The measurements were done in rotating apparatus. Platinum screen electrodes without diaphragms were used as counter-electrodes. The electrode potentials were measured, using a Haber-Luggin capillary, versus a mercury/mercury sulfate electrode at room temperature, and converted to the standard hydrogen scale. The experiments were done with the external potentiostatic circuit.

The samples were used air-passive at room temperature in the test solution, brought immediately to the desired experimental potential, and the electrolyte was warmed to the experimental temperature with nitrogen flushing. For Steels 1 and 2 the experimental times were between 4 and 24 hours, depending on the expected corrosion rates. For Steels 4 to 9 they were uniformly 24 hours. The polarization currents were recorded during the experiments. The corrosion rates were calculated from the corrosion losses determined by weighing after the experiments. Samples of the steels 6 to 9 were polished perpendicular to the plate surface to determine the nature of the attack, and the depth of the attack was determined.

In addition, the corrosion rates of Steels 1 and 3 were determined without the external current in 1% hydrofluoric acid at room temperature. The corrosion rates were calculated from

the corrosion losses of the steel samples determined by weighing after an experimental period of 24 hours.

4. Experimental Results

a) Steels X8Cr 17 and X8CrTi 17

Figure 5 shows the anodic partial current potential curve and the anodic total current potential curve of Steel 1 in 2 N H_2SO_4 determined from the corrosion losses in the potential range of E_H = -1000 to +200 mV. In the presentation of the

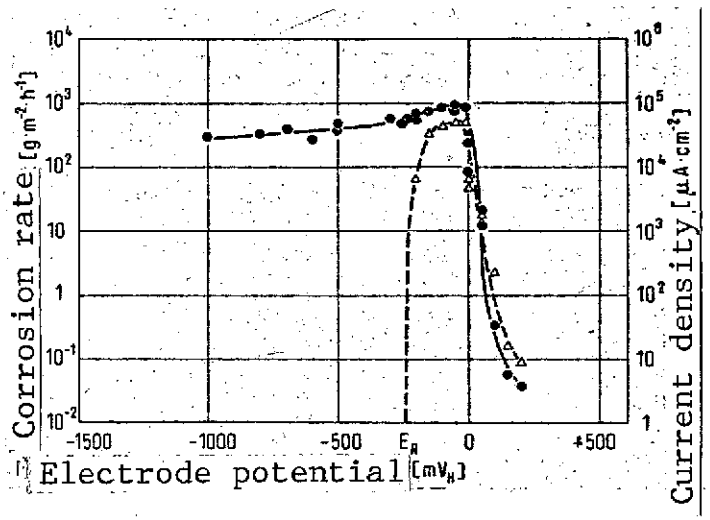

Figure 5. Corrosion rate (●——●) and polarization current density (△– – –△) of Steel 1 in 2 N H_2SO_4 (60°C) as functions of the electrode potential.

results of the electrochemical experiments, the plotting was always chosen so that the corresponding corrosion rates and dissolution current densities coincided according to the relation

$$10^{-2}\ g \cdot m^{-2} \cdot h^{-1} \triangleq 1\ \mu A \cdot cm^{-2}$$

which applies for the active dissolution of these steels.

The almost potential-independent plateau of the anodic partial current voltage curve extending over a wide potential range up to E_H = -25 mV is remarkable. Its boundary at non-noble potentials could not be determined because the cathodic control range of the potentiostat was reached. The corrosion rates in the potential range of this plateau are between 300 and 950 $g \cdot m^{-2} \cdot hr^{-1}$.

Between E_H = -25 mV and +200 mV, the corrosion rate drops by more than 4 orders of magnitude from about 950 $g \cdot m^{-2} \cdot hr^{-1}$ to 4 . 10^{-2} $g \cdot m^{-2} \cdot hr^{-1}$. The material changes from the active state into the passive state. The limit of the measurement accuracy was some 10^{-2} $g \cdot m^{-2} \cdot hr^{-1}$. For this reason, the corrosion rates plotted at this value could be even lower. The active-passive transition occurs, then, in a relatively narrow potential range of some 200 mV. Under the experimental conditions described the steel is "stable active". That is, it does not automatically transform into the passive state. The rest potential, E_R, measured without external current is at / 765
E_H = -235 mV. The matching corrosion rate is 600 $g \cdot m^{-2} \cdot hr^{-1}$. At more positive potentials, the measured current densities agree, to a good approximation, with the corrosion rates determined by weighing.

Figure 6 shows the measurements obtained with the Ti-stabilized Steel 2 in the potential range of E_H = -1200 to +200 mV. The anodic partial current voltage curve is approximately independent of the potential up to E_H = - 50 mV. The boundary of the plateau found with the non-noble potentials could not be determined. Up to E_H = -50 mV corrosion rates between 400 and 800 $g \cdot m^{-2} \cdot hr^{-1}$ were measured. In the range from E_H = -50 mV to +200 mV the corrosion rate falls by more

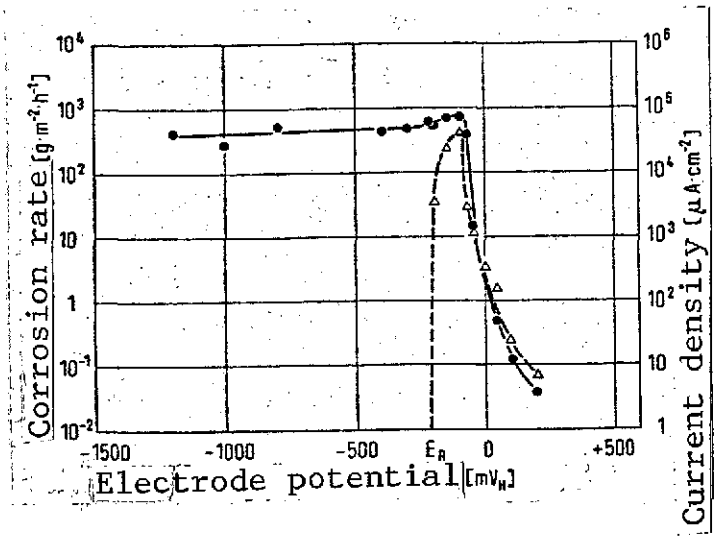

Figure 6. Corrosion rate (●——●) and polarization current density (△---△) of Steel 2 in 2 N H_2SO_4 (60°C) as functions of the electrode potential.

than 4 orders of magnitude to some 4 · 10^{-2} $g \cdot m^{-2} \cdot hr^{-1}$. Steel 2 is also "stable active" at the existing experimental conditions. The resting potential, E_R, measured without external current is at E_H = -210 mV. The matching corrosion rate is 600 $g \cdot m^{-2} \cdot hr^{-1}$. At more positive potentials the course of the anodic total current potential curve likewise matches that of the anodic partial current potential curve to a good approximation.

The rolled surfaces of both steels are attacked almost evenly in the entire potential region studied. The cut surfaces, on the other hand, are strongly pitted. This could be due to the microscopic segregations always present in the technological material.

No effect of Ti on the corrosion behavior in the active state was observed in the potentiostatic holding experiments. In order to test this result, the corrosion rates of the unstabilized Steel 1 and the two Ti-stabilized Steels 2 and 3

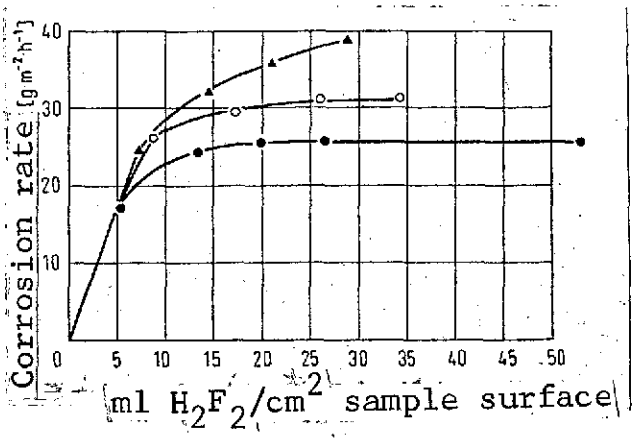

Figure 7. Corrosion rates of Steels 1 to 3 in 1% H_2F_2 at room temperature (average of 3 individual measurements).
●——● Steel 1
▲——▲ Steel 2
o——o Steel 3

were determined in still 1% hydrofluoric acid at room temperature, using three parallel samples of each. The chromium steels investigated are active in the hydrofluoric acid solution. In these experiments the effect of the ratio of electrolyte volume to sample surface was also studied. Figure 7 shows the experimental results. One notes first a distinct effect of the ratio of electrolyte volume to sample surface on the corrosion rate. As the corrosion rate increases, the numerical value of the ratio at which a corrosion rate independent of the electrolyte volume is reached also increases. The corrosion rates which are approximately independent of the electrolyte volume are between 24.5 $g \cdot m^{-2} \cdot hr^{-1}$ (Steel 1) and 39 $g \cdot m^{-2} \cdot h^{-1}$ (Steel 2). The corrosion rates show no dependence on the chromium content of the steels. In general, though, the corrosion rates of the Ti-stabilized steels are greater than those of the unstabilized steel.

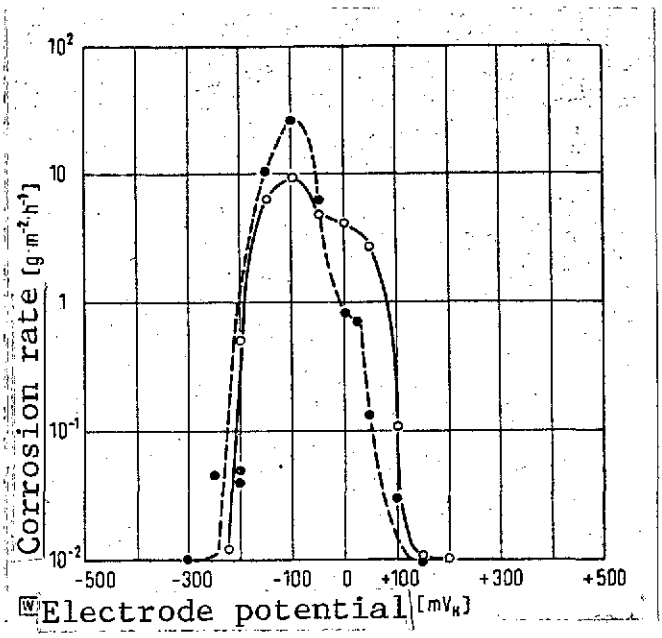

Figure 8. Corrosion rate of Steels 4 (○——○) and 5 (●——●) in 2 N H_2SO_4 as functions of the electrode potential.

b) Steels X5CrNi 18 9 and X10CrNiTi 18 9

Figure 8 shows the anodic partial current potential curves of the austenitic Steels 4 (unstabilized) and 5(Ti-stabilized). The plateau in the corrosion curve found for the ferritic chromium steels in the active state is no longer present. The potential range for the active corrosion is / 766
sharply limited with respect to non-noble potentials and begins at about E_H = -250 mV. There is a maximum for the corrosion rate at E_H = -100 mV. The maximum corrosion rates of Steels 4 (10 $g \cdot m^{-2} \cdot hr^{-1}$) and 5 (28 $g \cdot m^{-2} \cdot hr^{-1}$) differ by a factor of about 3. In the potential range of E_H = -100 mV to +150 mV the corrosion rates of both steels fall by about three orders of magnitude to values about 10^{-2} $g \cdot m^{-2} hr^{-1}$. In the potential range of E_H = -50 mV to +100 mV the corrosion rates of the unstabilized Steel 4 are generally distinctly increased in comparison to those of the Ti-stabilized Steel 5. Steel 5 is "stable passive" in 2 N H_2SO_4 at 60°C. No active rest

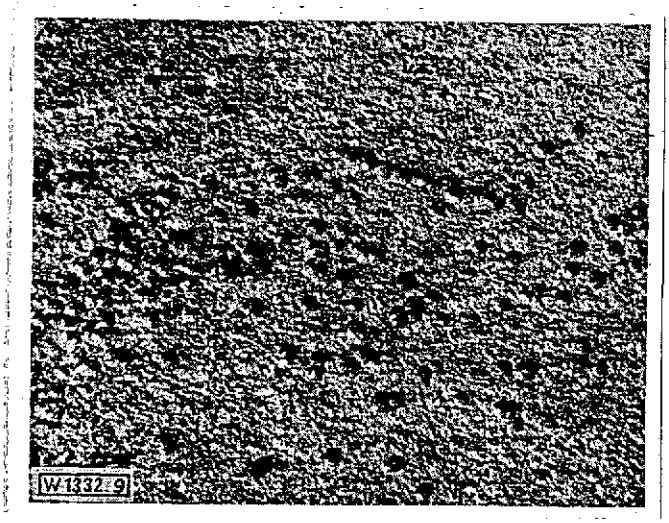

Figure 9. Development of flat pits on the surface of Steel 5 at E_H = -150 mV. 16:1.

potential is found even after previous activation of the steel by cathodic polarization. That is, the activated steel transforms automatically into the passive state. Presumably the residue of oxygen remaining in the electrolyte is sufficient for passivation. On the other hand, Steel 4 shows an active rest potential of E_H = -50 mV after previous activation.

Steels 4 and 5 also show almost general erosive corrosion attack. In agreement with previous experiments [2] in boiling 2 N H_2SO_4, development of flat pits could be observed with cathodic polarization at E_H = -150 mV, and a slight locally limited corrosion in the neighborhood of the platinum wire applied for current conduction in the range of cathodic protection.

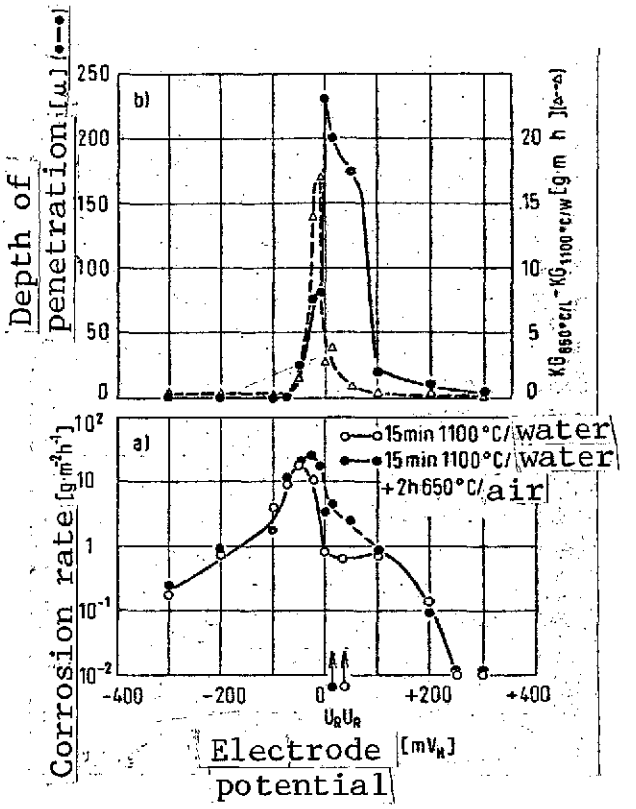

Figure 10. Corrosion rates of Steel 6 in the solution heat treated and sensitized states (a); penetration depth of the grain boundary attack in the sensitized state and difference of the corrosion rates in the two heat-treated states (b) as functions of the electrode potential.

c) Steel X5CrNiMoTi 25 25

Corrosion rate

The anodic partial current voltage curves measured for Steels 6 to 8 are shown in the lower parts of Figures 10 to 12. The points obtained after solution heat treatment, 100°C/water, are connected with solid lines, and those obtained after sensitization heating, 650°C/air, are connected by broken lines.

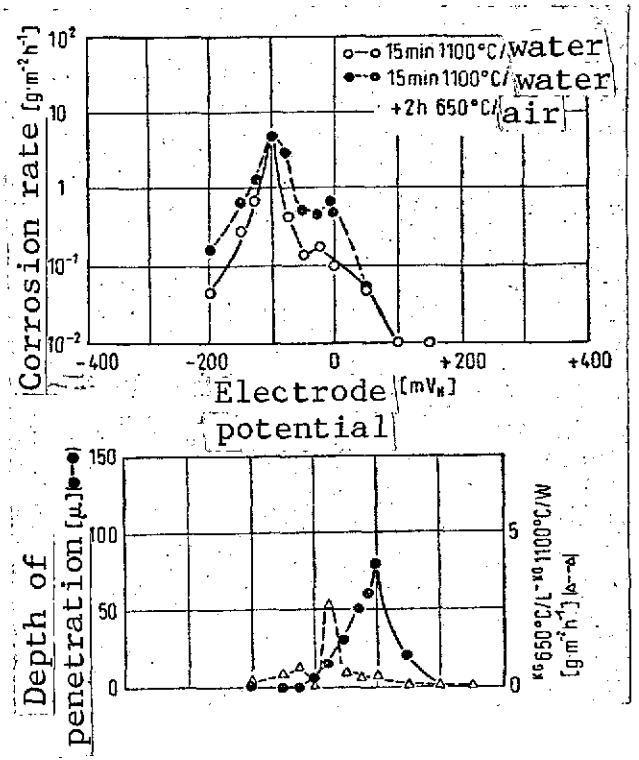

Figure 11. Corrosion rates of Steel 7 in the solution heat treated and sensitized states (a); penetration depth of the grain boundary attack in the sensitized state and difference of the corrosion rates in the two heat treated states (b) as functions of the electrode potential.

As for the Steels 4 and 5, a distinct maximum in the corrosion rate appears in the solution heat treated state at E_H = -50 to -100 mV (E_{max}). The maximum corrosion rate decreases from 19 $g \cdot m^{-2} \cdot hr^{-1}$ (Steel 6) to 2 $g \cdot m^{-2} \cdot hr^{-1}$ (Steel 8) as the stabilization ratio increases. At more noble potentials the corrosion rate passes through a secondary maximum which is shifted toward lower corrosion rates with rising stabilization ratio and is finally no longer found with Steel 8. The activation potential is displaced to more negative values with increasing stabilization ratio, from E_H = +250 mV (Steel 6) to E_H = -25 mV (Steel 3). At the active → passive transition

/767

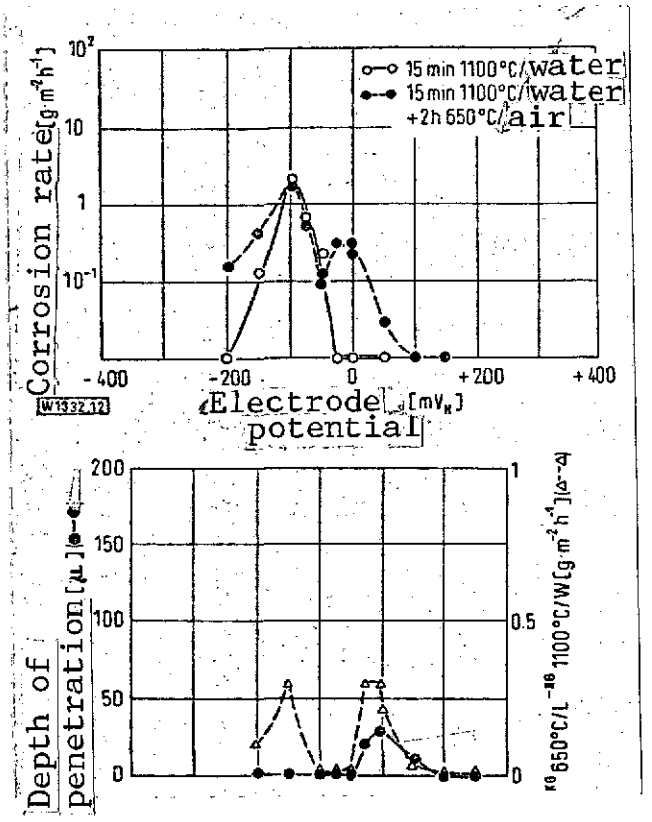

Figure 12. Corrosion rates of Steel 8 in the solution heat treated and sensitized states (a); penetration depth of the grain boundary attack in the sensitized state and difference of the corrosion rates in the two heat treated states (b) as functions of the electrode potential.

region the range of passive corrosion attaches itself to more positive potentials.

The corrosion rate at potentials less noble than E_{max} is also reduced with increasing stabilization ratio. The reduction of the corrosion rate in the active state with increasing stabilization ratio is expressed by the fact that Steel 6 is metastable active at the given experimental conditions (the rest potential U_R is at E_H = +63 mV in the active→passive transition), while the Steels 7 and 8 are stable passive.

In the sensitized state, almost the same maximum corrosion rate is attained by all steels as in the solution heat treated state. At potentials less noble than E_{max}, the corrosion rates of the sensitized samples are slightly increased over those of the solution heat treated samples for Steels 7 and 8.

The sensitization heating has a remarkable effect on the corrosion rate in the active→passive transition region. For all steels the corrosion rates of the sensitized samples are greater than those of the solution heat treated samples in a narrow potential range between -75 and +100 mV. In general the corrosion rate first decreases at potentials more positive than E_{max} and then passes through a secondary maximum which is at about E_H = 0 for all three steels. As the stabilization ratio increases, the corrosion rate is reduced, even in the sensitized state. The difference in the corrosion rates of the sensitized and solution heat treated states is plotted on the upper parts of Figures 10 to 12 (dashed curves).

Corrosion attack

Solution-heat-treated samples are evenly attacked. Sensitized samples suffer intercrystalline attack in the potential range of about -75 mV to +100 mV. This potential range coincides with the range in which the corrosion rate of the sensitized samples is increased with respect to that of the solution heat treated samples in the active-passive transition range [1]. The depths of attack for the intercrystalline corrosion are plotted on the upper parts of Figures 10 to 12 (solid lines). We can see the following relations:

---

(1) Steel 6 is an exception. It still shows a corrosion attack of slight depth even at E_H = +200 mV.

1. The maximum depth of attack decreases from 225 μ (Steel 6) to 30 μ (Steel 8) with increasing stabilization ratio.

2. The potential at which the strongest intercrystalline corrosion occurs is independent of the stabilization ratio and is between -25 mV_H and +25 mV_H in the potential range in which the corrosion rate of the sensitized steel passes through a secondary maximum.

3. The potential of the strongest intercrystalline attack does not coincide with the potential at which the difference of the corrosion rates in the sensitized and the solution heat-treated states is at a maximum, but is displaced to more positive values than this. Steel 8 is an exception. There the boundary of the active region from the anodic potentials is at -25 mV.

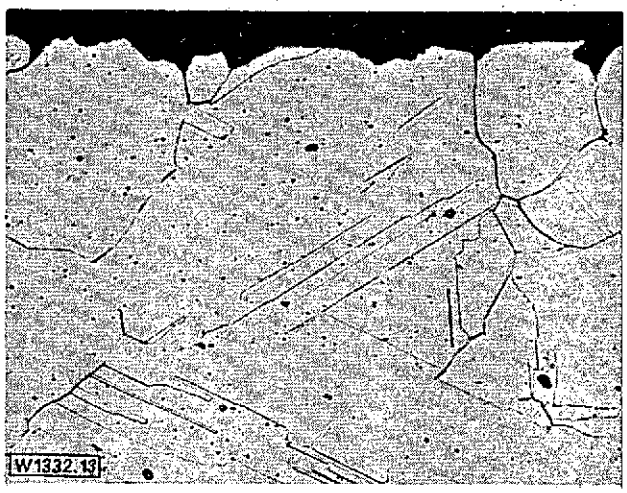

Figure 13. Incipient intercrystalline attack on Steel 6 (sensitized 2 hours 650 °C/air) at E_H = -50 mV. 200:1. V2A etchant.

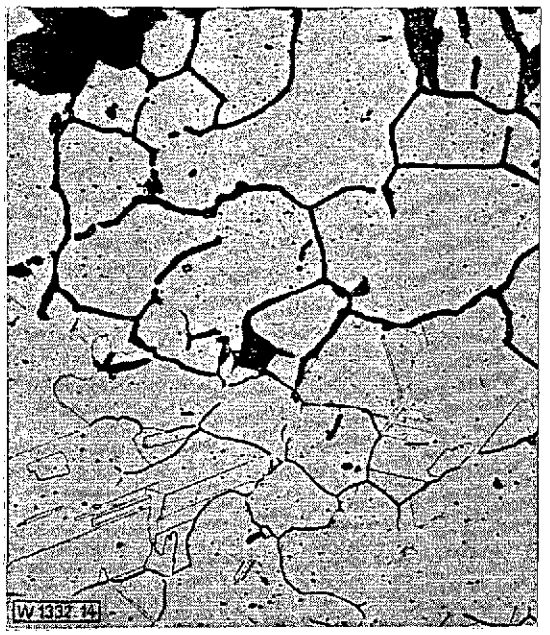

Figure 14. Maximum of the intercrystalline attack on Steel 6 (sensitized 2 hours 650°C/air) at E_H = 0 mV. 200:1. V2A etchant.

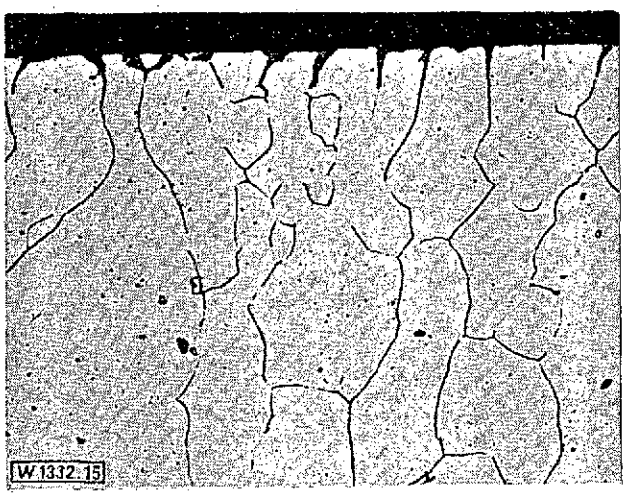

Figure 15. Decreasing intercrystalline attack on Steel 6 (sensitized 2 hrs 650° C/air) at E_H = 100 mV. 200:1. V2A etchant.

Figures 13 to 15 show examples of the intercrystalline corrosion attack on sensitized Steel 6 for the potentials E_H = -50 mV (beginning attack), E_H = 0 mV (maximum attack) and E_H = +100 mV (decreasing attack, compare Figure 10). /768

The anodic partial current potential curve of the solution heat treated Steel 9 is nearly identical with the corresponding curve for Steel 7 (Compare Figure 11). After a sensitizing heating (2 hours, 650 °C/air) the corrosion rates are somewhat increased in comparison with the solution heat treated state for Steel 9, but the active corrosion in the entire potential range studied is only generally erosive, with no intercrystalline attack.

Etching behavior and testing for frequency of grain loss

Steels 6 to 9 are active in the usual hydrochloric acid-nitric acid etchant (composition: 1000 ml H_2O, 1000 ml conc. HCl, 100 ml conc. HNO_3; etching temperature 60°C) used for etching stainless steels. The corrosion potential is between -60 and -50 mV_H. Solution heat treated samples are attacked evenly in this etchant. The corrosion potential for sensitized samples (-70 mV_H) differs only slightly from that of the solution heat treated steels. But in the sensitized state there is intercrystalline attack (Figure 16). The strength of the intercrystalline attack in the etchant was determined by means of potentiostatic experiments in the potential range from E_H = +150 mV to E_H = -450 mV. Intercrystalline corrosion occurs over the entire range. The maximum depth of attack is at E_H = -150 mV. This explains why sensitized steels of the type X5CrNiMoTi 25 25 cannot be etched even in modified nitric-hydrochloric etches with increased or decreased acid concentration or in nitric acid-hydrofluoric acid etches without intercrystalline attack occurring, as the corrosion potential is in the active or in the active-passive transition region in these etches.

Figure 16. Grain boundary attack in Steel 6 (heat treatment 15 min. 1100 °C/air + 2 hrs 650 °C/air) in nitric-hydrochloric etchant (etch duration 60 minutes, etch temperature 60°C). 500:1. V2A etchant.

Therefore the heating scale must be removed by polishing in the study of the potential dependence of the intercrystalline attack. This is also necessary if the frequency of grain loss is to be tested with the Strauss test.

The Strauss solution, like the test solution used in the electrochemical experiments, is 2 N in sulfuric acid. The test potential is E_H = +350 mV. The testing in the Strauss test differs from the potentiostatic investigations described above through the reduced test duration (15 hours) and the increased test temperature (boiling temperature). The testing in the Strauss test is sharper in respect to the latter condition, and milder with respect to the position of the test potential.

In the Strauss test, only sensitized samples (2 hrs 650°C/air) of Steel 6 undergo intercrystalline attack of slight depth (~ 5 µ). The sensitized Steels 7 to 9 do not.

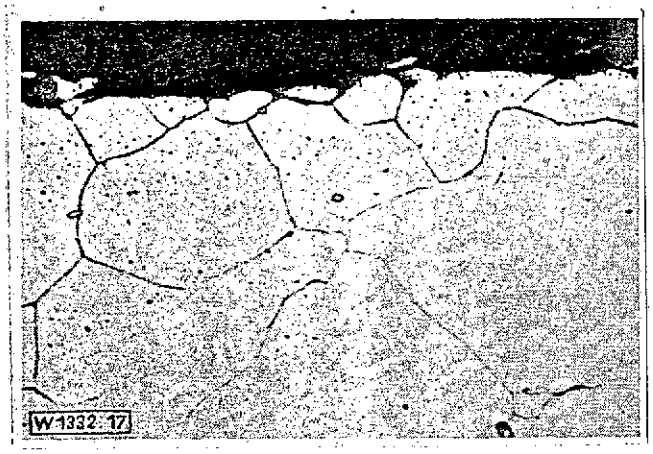

Figure 17. Intercrystalline corrosion attack on Steel 6 in the Strauss test after heat treatment of 15 min 1100°C/water + 2 hrs 650°C/air and removal of the heating scale by polishing.

5. Discussion of the Experimental Results

Ti as an alloying element has no detectable effect on the active corrosion of ferritic 17% chromium steels in sulfuric acid. According to the corrosion experiments performed in 1% hydrofluoric acid, addition of titanium increases the corrosion rate of these steels in this corrosive agent.

On the other hand, a reduction of the corrosion rate with Ti is observed for austenitic 18-8 Cr-Ni steels in the active→passive transition range and at the rest potential. This finding agrees with the experimental results of E. Brauns et al. [7], by which the corrosion rate of a steel containing 0.057% C, 17.94% Cr and 10.15% Ni at the rest potential in boiling 1 N H_2SO_4 is 22 $g \cdot m^{-2} \cdot hr^{-1}$, while that of a steel containing 0.09%C, 18.24% Cr, 9.44% Ni and 0.59% Ti under the same conditions is 15 $g \cdot m^{-2} \cdot hr^{-1}$. Apparently the effect of Ti is expressed more strongly in the austenitic chromium-nickel steels than in ferritic chromium steels. Two effects which

are strongly expressed with Steel X5 CrNiMoTi 25 25 can already be observed, as suggestions, in the Cr-Ni steels of the 18-8 type. These are the shift of the active-passive transition range to less noble potentials and the narrowing of the active range. If we consider that the corrosion rate of the titanium-stabilized Steel 5 is reduced in the active-passive transition range and that this steel has no active rest potential, in contrast to the titanium-free Steel 4, then we also find agreement with Ya. M. Kolotyrkin [8], that the critical passivation current density is reduced and the transition into the passive state is facilitated in austenitic stainless chromium-nickel steels by addition of Ti. In this relation, K. Bungardt and H.-J. Rocha [9] indicate that a strong titanium effect can be determined in steels of the 18-8 type only if there is no Mo in the steel. Even the unintended slight Mo content in 18/9 CrNi steel of commercial melting eliminates the Ti effect. By plotting current density - potential curves in sulfuric acid, however, the effect of the Ti could be demonstrated and accurately differentiated even in the presence of 0.3% Mo.

The facilitated transition into the passive state in the titanium-containing steels does not contradict the experimental finding that the maximum corrosion rate of the Ti-stabilized steel is greater than that of the unstabilized steel, as this cannot be equated with the passivation current density. The corrosion rate of stainless austenitic steels in sulfuric acid increases with cathodic polarization and reaches a maximum at about E_H = -100 mV. The "active hump" in the current potential curve is not characteristic for the active range. Rather, it is found in the less significant part of the active range, namely, in the active-passive transition range, on the investigation of the potential dependence of the corrosion rate [3].

From this we can draw the important conclusion that the cathodic protection of stainless steels in acids is problematic. In this work it was shown that the last-mentioned findings are also applicable for ferritic 17% chromium steels. In these steels, too, the active hump is in the active-passive transition range and says nothing about the extension of the active range for corrosion. Rather, the limit of this active range on the cathodic side should be sought at potentials which are less noble than the active resting potential by more than 1 V.

The development of a distinct plateau in the corrosion rate of the ferritic Cr steels in the active state appears particularly interesting. Such a plateau is also found with austenitic 18-8 Cr-Ni steels in sulfuric acid flushed with SO_2 and H_2S [3, 5]. In all the cases mentioned, with comparable experimental conditions in respect to sulfuric acid concentration and temperature, the corrosion rates are in the same order of magnitude, that is, $5 \cdot 10^2$ to $8 \cdot 10^2$ $g \cdot m^{-2} \cdot hr^{-1}$. In contrast, no plateau in the corrosion rate is observed in solutions free of SO_2 of H_2S [3, 5]. Only a maximum appears in the corrosion rate, but the corrosion rates are of the order of 5 to 10 $g \cdot m^{-2} \cdot hr^{-1}$, about 2 orders of magnitude smaller than in the former cases.

The development of a plateau in the active range is very distinct, particularly for pure iron in sulfuric acid [10]. In this case, the diffusion-controlled dissolution of an iron sulfate coating on the sample surface determines the maximum corrosion rate. If a similar mechanism occurs in the alloyed steels, then Cr and Ni should have no significant effect on the development and height of the plateau. As the present studies at +60°C show, this applies for Cr, as the corrosion rate of the ferritic 17% Cr steels is in the same order of magnitude as that of pure Fe in sulfuric acid, and is only slightly lower than that [11]. On the other hand, addition of Ni prevents the development of an active plateau and also

reduces the maximum corrosion rate in the active state [3]. This signifies that effects other than the dissolution of a salt coating are effective for the active corrosion of Ni-alloyed steels (1). It can be assumed that the previously unknown effect of Ni on the corrosion mechanism of austenitic Cr-Ni steels in the active state is eliminated by hydrogen sulfide and sulfur dioxide. /770

The titanium effect is significantly more distinct in steels of the type X5 CrNiMoTi than with the 18-8 type. The corrosion rate of these steels in the active state in sulfuric acid is reduced by increasing contents of titanium. The active-passive transition range is shifted to less noble potentials and the active range is narrowed. The same effect has previously been observed [3] in steels of the 18-8 type with increasing Mo contents, but the effect of Ti is significantly greater in steels of the type X5 CrNiMoTi 25 25. Here, an increase in the Ti content from 0.41 to 0.66% reduces the maximum corrosion rate from 19 to 2 $g \cdot m^{-2} \cdot hr^{-1}$. For steels of the 18-8 type, by comparison, the maximum corrosion rate is reduced only from 14 $g \cdot m^{-2} \cdot hr^{-1}$ (0.25% Mo) to 4 $g \cdot m^{-2} \cdot hr^{-1}$ (2.30 to 4.20% Mo) [3].

Steels of the 25-25 type with C contents of about 0.06% and Ti contents between 0.41 and 0.66% are still susceptible to intergranular corrosion after sensitization heating of 2 hours 650°C/air. The severity of this susceptibility to grain loss

---

(1) It was concluded from previous studies [3] that the reduction of the corrosion rate in the active state is caused principally by Mo. It is more probable, however, that the reduction of the maximum corrosion rate in the active state is caused by Ni, while Mo apparently predominantly reduces the corrosion rate in the active-passive transition range, thus facilitating the ability to passivate the stainless Cr-Ni steels.

generally decreases with increasing Ti content. At times, support is expressed for the view that the condition: % Ti > 5 x %C is sufficient to ensure resistance to grain loss [1]. Because of the formation of titanium nitride, however, the N content must also be considered in determining a suitable stabilization ratio. Theoretically, a steel with a Ti content of 4 x %C + 3.5 x %N must be capable of complete stabilization, so that 0.31% should suffice for Steels 6 to 8. But this is not the case.

Susceptibility to intergranular corrosion in highly alloyed steels in the active-passive transition range after sensitizing heating is based on the precipitation of chromium-rich carbides of the type $(Fe,Cr)_{23}C_6$ at the grain boundaries, with resulting chromium depletion in their vicinity [12]. Electron diffraction studies with Steel 6 indicate that they are also dealing with carbides of the type $M_{23}C_6$ precipitated at grain boundaries of sensitization-heated samples. But it is not certain whether only carbides of the type mentioned are present as precipitates, because there is strong attack at the grain boundaries on etching of the sensitized samples in nitric-hydrochloric acid etchant and the corrosion products remaining in the depressions make the evaluation of the diffraction pattern difficult.

B. Hattersley and W. Hume-Rothery [13] investigated Fe-Cr-Ni-Ti alloys with Ni contents between 24 and 30% Ni and Cr contents between 17 and 34% Cr. The C contents were 0.023 to 0.068%. One series of alloys contained 0.3% Ti, and another series 0.7% Ti. The chromium-rich carbide was isolated by chemical dissolution of the alloys in a solution of 5% bromine

---

(1) As an undesired linear development of titanium carbo-nitrides occurs at high Ti contents, the maximum titanium content is often limited by the condition Ti < 5 x %C + 0.2.

in methanol or in 5% hydrochloric acid. It appeared that in spite of the great affinity of Ti to C and N, $(Cr,Fe)_{23}C_6$ was found after heating at temperatures below 950°C for all alloys with 0.3% Ti $\left(\frac{\%\,Ti}{\%\,C + \%\,N} = 4{,}5 - 7{,}5\right)$ and for most of the alloys with 0.7% Ti $\left(\frac{\%\,Ti}{\%\,C + \%\,N} = 8{,}4 - 12{,}0\right)$. At least in the alloy series with 0.7% Ti, the Ti content in each case exceeds that amount required for binding the C and N (1).

The requirement for a certain stabilization ratio does not, however, ensure that steels of the type X5 CrNiMoTi 25 25 will be resistant to grain loss after sensitizing heating. In addition, the absolute magnitude of the carbon content plays a part. Steel 9 in this study, with 0.03% C $\left(\frac{\%\,Ti}{\%\,C + \%\,N} = 6{,}3\right)$ is resistant to intergranular corrosion in the studies described, but Steel 7 is not, in spite of the fact that the stabilization ratio is approximately the same $\left(\frac{\%\,Ti}{\%\,C + \%\,N} = 6{,}6\right)$. Therefore, we can only say with certainty that steels of the type X5 CrNiMoTi 25 25 are resistant to grain loss after sensitization heating for 2 hours at 650°C/air with C contents of 0.03% if the ratio $\frac{\%\,Ti}{\%\,C + \%\,N} \geq 6{,}6$ is maintained, and that an increase of the C content at the same stabilization ratio places the resistance to grain loss in question.

---

(1) In studies by M. Deighton [14] on the solubility of NbC in 20% Cr - 25% Ni steels it was shown that $M_{23}C_6$ still occurs after heat treatment of 48 hours 700°C/air even in niobium-stabilized steels with carbon contents of about 0.075%, in spite of a stabilization ratio of $\frac{\%\,C + \%\,N}{\%\,Nb} = 7{,}2$.

In studies on a sensitized steel of the type X5 CrNi 18 9 in boiling 2 N H_2SO_4, normal intercrystalline corrosion was found in a potential range of E_H = +200 to +1150 mV (1) [15]. The maximum attack was at potentials more noble than E_H = +100 mV. For 18-8 CrNi steels, the Strauss test is entirely sufficient to demonstrate susceptibility to intergranular corrosion. At the same time it was established that although sensitized steels of the type X5 CrNi 18 9 undergo a severe general attack, they experience no preferential attack at the grain boundaries [15].

Sensitized steels of the type X5 CrNiMoTi 25 25 show a different behavior. The severity of the intercrystalline attack also depends on the electrode potential, of course, but it has a sharply developed maximum at 0 mV_H.

The potential range for this attack is very narrow in 2N H_2SO_4 at 60°C. It lies between -75 mV_H and +100 mV_H, so that it is at a considerably less noble potential than the range of the intercrystalline attack on 18-8 Cr-Ni steels. / 771

For this reason, the Strauss test is not suitable for testing resistance to grain loss in steels of the type X5 CrNiMoTi 25 25. The redox potential of the Strauss solution is E_H = +350 mV, so that it is some 350 mV more positive than the potential for the range of intercrystalline attack.

In contrast to 18-8 Cr-Ni steels, sensitized steels of the type X5 CrNiMoTi 25 25 experience intercrystalline corrosion in nitric-hydrochloric acid etchant. The rest potential of both steels in the etchant are at E_H = -50 to -100 mV. But at these

(1) At less noble potentials there is an attack called "internal pitting". At more noble potentials even non-sensitized samples experience a furrow-like attack.

potentials only 25-25 Cr-Ni steels, and not 18-8 Cr-Ni steels, are subject to intercrystalline attack in the sensitized state.

There is, finally, the question of why the potential range for intercrystalline corrosion is at considerably less noble potentials for sensitized steels of the type X5 CrNiMoTi 25 25 in comparison to sensitized 18-8 Cr-Ni steels. From the standpoint of the chromium depletion theory, it must be assumed that the current density - potential curves for the dissolution of metal from the chromium-depleted regions at the grain boundaries and from the undepleted grain surfaces differ only in a narrow potential range at relatively negative potentials, i. e., the range of intercrystalline corrosion. In contrast to sensitized 18-8 Cr-Ni steels, this could be applicable only for sensitized Cr-Ni steels with high chromium contents. That is, the chromium content in the chromium-depleted regions must be significantly higher than in the 18-8 Cr-Ni steels.

There are insufficient reports on the interesting quantities, activation potential or the position of the active-passive transition and the magnitude of the corrosion rates in the active and passive state for Cr-Ni steels with high Cr contents. From an investigation by H.-J. Rocha and G. Lennartz [16], we learn that the activation potential of FeCr alloys changes only slightly with the chromium content for chromium contents between 18 and 20%. The activation potential for such alloys is in the same order of magnitude as the potential range in which sensitized steels of the 25-25 type suffer intercrystalline attack. This slight dependence of the activation potential on the Cr content explains why the steels investigated show intercrystalline attack only in a very narrow potential range. Here there is corrosion attack of the active-passive type [15]. Intercrystalline corrosion of the active-active and passive-passive types, which are characterized by a considerably

smaller depth of attack, could essentially occur at all other potentials. But no statements can be made about the extent of the corrosion attack of these types, because the dependence of the corrosion rates on the Cr content in the active and passive states is not known.

The strong dependence of the corrosion rate and of the active-passive transition on the Ti content, described in this report, can likewise be used to explain the susceptibility to intercrystalline attack. If, in the sensitizing heating, not only chromium carbide of the type $M_{23}C_6$ but also titanium carbonitride of the type M(C,N) is precipitated at the grain boundaries, then titanium depletion, corresponding to the chromium depletion, should also occur in the grain boundary region. The effects of titanium depletion should correspond to those of chromium depletion. We cannot determine from the existing experimental results the extent to which a titanium depletion contributes to intercrystalline corrosion. More detailed testing could be difficult, because the titanium depletion is always superimposed on a chromium depletion.

6. Summary

In this work, the effect of the titanium content on the corrosion of steels of the type X8 Cr 17 (X8 CrTi 17), X5 CrNi 18 9 (X10 CrNiTi 18 9) and X5 CrNiMoTi 25 25 in the active state in sulfuric acid (60°C) is studied by potentiostatic holding experiments. The following results were obtained:

1. In ferritic 17% chromium steels, a titanium content on the order of that usually added to stabilize these steels (% Ti > 7 x %C) has no effect on the corrosion rate in the active state in sulfuric acid. The position of the active-passive transition range and the potential range of active dissolution are likewise not affected. In these steels the

corrosion rate in the active state is independent of the electrode potential over a wide potential range.

2. In austenitic molybdenum-free 18-8 Cr-Ni steels, the corrosion rate in the active-passive transition range and the passivation current density are reduced with titanium as the stabilizing element. The transition from the active to the passive state is also facilitated. The corrosion rate at first increases with cathodic polarization. A distinct maximum in the corrosion rate appears at E_H = -100 mV. Ti has only a very slight effect on the maximum corrosion rate and on the extent of the active range of corrosion.

3. In solution heat treated steels of the type X5 CrNiMoTi 25 25, the corrosion rate in the active state is reduced by increasing titanium content, and the potential range for active corrosion is narrowed. The steels studied in this state are generally attacked by over-all removal of material, independently of the titanium content.

In the sensitized state the corrosion rates of these steels with carbon contents of some 0.06% C and titanium contents of 0.41 to 0.66% Ti are increased, in comparison to the solution heat treated state in the active-passive transition range. There is intercrystalline attack in this range. The severity of the grain loss decreases with increasing stabilization ratio $\frac{\%\,Ti}{\%C + \%N}$. The potential range for intercrystalline attack is very narrow, about 200 mV. The depth of the attack has a distinct maximum at 0 mV_H. Aside from the stabilization ratio, the sensitization also depends on the absolute magnitude of the carbon content. No intercrystalline corrosion attack was found after sensitizing heating at a stabilization ratio of $\frac{\%\,Ti}{\%C + \%N} = 6{,}3$. /772

The steels of types X5 CrNiMoTi 25 25 and X5 CrNi 18 9 are compared with respect to their behavior in the sensitized state and their corrosion properties are discussed from the standpoint of the chromium depletion theory.

REFERENCES

1. Engell, H.-J. and T. Ramschandran. Z. physik. Chemie. Vol. 215, 1960, pp. 176 - 184.

2. Schwenk, W. Werkstoffe und Korrosion. Vol. 14, 1963, pp. 646 - 657.

3. Herbsleb, G. and W. Schwenk. Werkstoffe und Korrosion. Vol. 18, 1967, pp. 521 - 529.

4. Brauns, E., W. Schwenk and H.-E. Bühler. Stahl und Eisen. Vol. 84, 1964, pp. 790 - 798.

5. Herbsleb, G. and W. Schwenk. Werkstoffe und Korrosion. Vol. 17, 1966, pp. 745 - 750.

6. Ijzermans, A. B. and A. J. van der Krogt. Corrosion Sci. Vol. 9, 1968, pp. 679 - 687.

7. Hume-Rothery, W. et al. Journ. Iron Steel Inst. Vol. 145, 1942, pp. 129 - 141.

8. Kuyazheva, V. M., Ya. M. Kolotyrkin, M. A. Vedeneeva and R. S. Ramazanova. Khim. prom. Vol. 5, 1964, p. 381.

9. Bungardt, K. and H.-J. Rocha. Corrosion behavior of passivatable steels in solutions. Lecture. Fourth Congress of the European Coal and Steel Community, Luxemburg, July 9 - 11, 1968.

10. Bartlett, J. H. J. Electrochem. Soc. Vol. 87, 1945, p. 521. Bartlett, J. H. and L. Stephenson. J. Electrochem. Soc. Vol. 99, 1952, p. 504.

11. Herbsleb, G. Dissertation, Bonn, 1963.

12. See also: A. Baumel, H.-E. Buhler, H.-J. Schuller, P. Schwaab, W. Schwenk, H. Ternes and H. Zitter. Corrosion Sci. Vol. 4, 1964, pp. 89 - 103.

13. Hattersley and W. Hume-Rothery. J. Iron Steel Inst. Vol. 204, 1966, pp. 683 - 701.

14. Deighton, M. J. Iron Steel Inst. Vol. 205, 1967, pp. 535 - 538.

15. Schuller, H.-J., P. Schwaab and W. Schwenk. Arch Eisenhüttenwes. Vol. 33, 1962, pp. 853 - 868.

16. Rocha, H.-J. and G. Lennartz. Arch. Eisenhüttenwes. Vol. 26, 1955, pp. 117 - 123.

Translated for National Aeronautics and Space Administration under Contract No. NASw 2483, by SCITRAN, P. O. Box 5456, Santa Barbara, California, 93108.